Journal of Low Temperature Physics (2021) 202:418–430
https://doi.org/10.1007/s10909-020-02546-8

Generation and Demolishment Mechanisms of Vapor Bubble Around Hot Tungsten Filament in Superfluid Helium-4

Che-Chi Shih[1] · Ming-Huei Huang[1] · Pang-Chia Chang[1] · Po-Wei Yu[1] · Wen-Bin Jian[1] · Kimitoshi Kono[2,3,4]

Received: 25 August 2020 / Accepted: 20 November 2020 / Published online: 7 January 2021

Abstract

The electric transport *I*–*V* characteristics of a tungsten filament immersed in superfluid helium are experimentally studied. The forward sweep *I*–*V* characteristics show an abrupt jump from the linear ohmic regime (*C* state) to the high-resistance non-ohmic regime (*H* state). In the *H* state, the filament is covered with a He gas bubble. In the *C* state, there is no gas bubble, that is, liquid He directly touches the filament surface. The transitions between these two states exhibit a well-developed hysteresis and bistability. The transition from the *H* state to the *C* state occurs at the equilibrium gas–liquid phase transition point, as reported by Date et al. (J Phys Soc Jpn 35(4):1190, 1973), whereas the *C*-to-*H*-state transition occurs in the superheat region.

Keywords Superfluid helium · Phase transition · Hot tungsten filament · Bubble formation

✉ Che-Chi Shih
a271711@hotmail.com

Kimitoshi Kono
kkono@nctu.edu.tw

[1] Department of Electrophysics, National Chiao Tung University, Hsinchu 300, Taiwan

[2] International College of Semiconductor Technology, National Chiao Tung University, Hsinchu 300, Taiwan

[3] RIKEN CEMS, Hirosawa 2-1, Wako-shi 351-0198, Japan

[4] Institute of Physics, Kazan Federal University, Kazan, Russia 420008

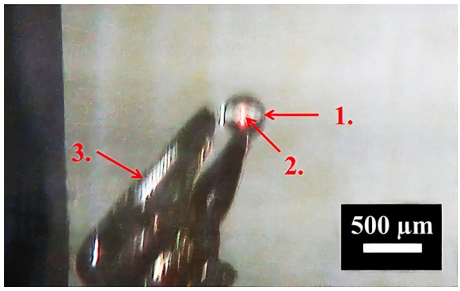

Fig. 1 (Color figure online) Image of glowing filament in superfluid: 1. He gas bubble, 2. glowing filament, 3. broken glass cover. The applied voltage is 0.8 V with current of 0.014 A at 1.526 K and at 4 cm in depth

1 Introduction

A hot tungsten filament is a versatile electron source essentially used for producing electron bubbles inside liquid helium [1] and surface state electrons on a liquid helium surface [2]. Electrons in a metal can have sufficient energy to overcome the work function when the metal is heated, namely, thermionic emission. When the filament is used under cryogenic conditions, some precaution is necessary because the electric transport becomes strongly nonlinear. However, the electrical and thermal transport characteristics of a hot tungsten filament in liquid helium are rarely investigated.

A tungsten filament submerged in liquid helium can still be heated to glowing temperature of about 1000 to 2000 K even when the liquid helium becomes superfluid with an extremely high thermal conductivity below the λ-point. The phenomenon is due to the formation of a He gas bubble covering the filament, as shown in Fig. 1. A glowing filament is a common demonstration of the extremely high thermal conductivity of superfluid ^{4}He. As long as the electric bias condition for the filament is moderate such that superfluid He efficiently carries away the Joule heat produced from the filament surface, the filament temperature remains low and no gas bubble appears around the filament. Hereafter, we refer to this state as the cold state (C state). Gas bubbles are eventually formed by varying the bias condition to increase heat production. Inside a gas bubble, the filament temperature increases rapidly because of the poorer thermal conductivity of He gas than of liquid He, and the filament starts to glow. This state with the He gas bubble is hereafter referred to as the hot state (H state). Schematic images of the C and H states are shown in Fig. 2a, b, respectively. One can understand that the transition between the C and H states must be closely associated with the gas–liquid phase transition.

A strong nonlinear electric transport due to the He gas bubble was reported by Date et al. decades ago [3]. They explained the bubble formation transition on the basis of an equilibrium gas–liquid phase diagram. With a large heat flow from the filament, a thin boundary layer is formed in which a finite temperature gradient is confined. Outside this layer, the heat transport is due to a thermal counterflow, and only a significantly small temperature gradient builds up. Inside the layer, the diffusion of quasiparticles (phonons and rotons) accounts for the heat transport, as described by Khalatnikov [4]. The temperature of liquid He adjacent to the filament (T_0) is higher than the ambient temperature T_1 of superfluid He. It was assumed that

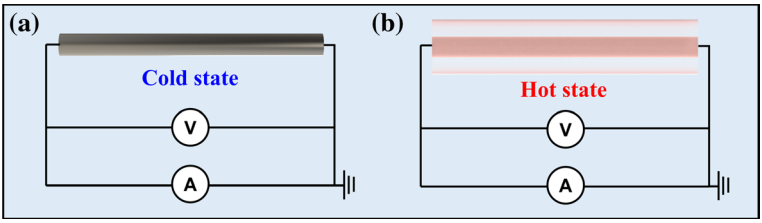

Fig. 2 (Color figure online) **a** Schematic of a tungsten filament in cold state (*C* state). **b** Schematic of a tungsten filament covered with the helium gas sheath in hot state (*H* state)

a vapor sheath along the filament appeared when T_0 reaches the gas–liquid phase transition temperature under excessively high pressure because of the finite depth or pressure head of liquid helium. Although a hysteresis was observed in previous works [3, 5], only the mechanism of above-mentioned equilibrium gas–liquid phase transition was discussed. To properly explain the hysteresis, it is necessary to consider the superheat limit as well.

In this study, we experimentally investigated the electric transport *I*–*V* characteristics of a tungsten filament, which was prepared from a commercial light bulb. The *I*–*V* characteristics show an abrupt current jump in a forward sweep of bias voltage. This jump does not depend on the depth or pressure at the filament position. During the transition, the power density (heat flux) is one order of magnitude higher than the previously reported values [3, 5]. As for the backward sweep, the transition from the *H* state to the *C* state is smooth and the power density is closer to the previously reported values. The backward sweep transition does depend on the depth as previously reported [3, 5].

We analyzed the observed backward sweep critical behavior of *H*-to-*C*-state transitions on the basis of the model developed by Date et al. [3]. The model successfully explains our observations in the backward sweep. As for the forward sweep, the model cannot explain our experimental results. Therefore, we extrapolate the backward sweep results to evaluate the superheat limit.

2 Experimental Methods

As reported previously [6], to prepare tungsten filament samples in direct contact with liquid helium, the glass covering was removed from miniature light bulbs (Micro-Glühlampen-Gesellschaft, Hamburg, Germany). Then, four leads were connected to the tungsten filament samples for four-wire measurements. The *I*–*V* characteristics were obtained using a Keithley 2400 source meter with a waiting time of 100 ms for each step. The steady current state of filament was confirmed by employing different waiting time up to 1 s, which shows same results as 100 ms. The lowest temperature of this cryostat is 1.331 K.

A scanning electron microscope (SEM) system (JEOL IT-300) was utilized to observe the tungsten filament [6], which is suspended and anchored to two metal leads. The filament was wound to a coil shape. To identify the geometrical

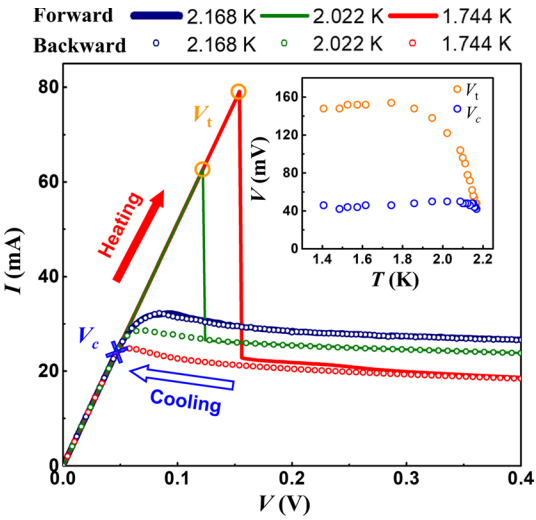

Fig. 3 (Color figure online) *I–V* characteristics of a tungsten filament in superfluid helium. The lines indicate the forward sweep of the voltage from 0 to 0.4 V, and the open circles indicate the backward sweep of the voltage at different temperatures at a depth of 4 cm. The orange circles and the blue cross indicate the transition voltage (V_t) and the critical voltage (V_c), respectively. The inset shows V_t and V_c as functions of temperature

characteristics of the tungsten filament, we obtained SEM images of several tungsten filament samples from the same batch whose average radius of the coil was measured to be 12.26 ± 0.49 μm. By calculating the number of coil turns and the filament length outside the coil, we estimate the total length to be 3.06 ± 0.07mm. Moreover, the average diameter of the tungsten filament was determined to be 3.97 ± 0.03 μm. The average total surface area of the filament was estimated to be 0.0382 ± 0.0008 mm^2.

3 Results and Discussion

Figure 3 shows the *I–V* characteristics of the tungsten filament sample with forward and backward sweeps between 0 and 0.4 V at different temperatures. The *I–V* loops consisted of heating up (forward) and cooling down (backward) processes. The depth of the sample from the liquid helium surface was fixed at 4 cm to maintain the same pressure. In the temperature range above or close to T_λ, the *I–V* characteristics of heating up and cooling down shown as blue traces in Fig. 3 almost overlap. A similar behavior was observed in vapor phase helium [7]. However, the hysteretic properties start to be observed at temperatures below about 2.135 K. The forward and backward sweeps deviate from each other in a certain voltage region. The behavior implies significantly different states of heating and cooling processes in this range.

Both forward and backward sweeps show linear behavior in the low-voltage region, which have the same resistance of about 1.95 Ω from 2.168 to 1.406 K as shown in Fig. 3. In the forward sweep, we define the *transition* voltage V_t as the value when $\mathrm{d}I/\mathrm{d}V$ drops below 95 % of the linear region. In the backward sweep, the *critical* voltage V_c is the value at which the system returns to the linear region, which was determined by employing the same 95 % $\mathrm{d}I/\mathrm{d}V$ criterion. The difference

between V_t and V_c is the hysteresis window. Note that V_t is always larger than V_c. The inset of Fig. 3 shows that V_t increases as temperature decreases. On the other hand, V_c is almost constant (46 mV) at different temperatures. Hence, the hysteresis window also gradually increases and finally saturates at about 100 mV with power density difference of about 0.282 $\mathrm{Wmm^{-2}}$ below 1.8 K. Note that the *I–V* characteristics show a negative differential resistance at voltages higher than V_t and V_c, which was also typically observed during filament heating in He gas vapor [7].

As the voltage increases beyond V_t, the superfluid near the tungsten filament vaporizes and detaches from the tungsten filament surface. Because of the low thermal conductivity of helium vapor, once a vapor bubble emerges in a certain area of the filament surface, the temperature of this area immediately increases. Then, the local vapor bubble eventually surrounds the entire filament as a spherical bubble. In the *H* state, no boiling bubble forms because the temperature is uniform throughout the superfluid.

In the *H* state, heat is generated from the surface of the filament and transferred to the liquid by helium gas inside the bubble. The bubble is supported by the joule heat produced from the tungsten filament, the mechanism of which is discussed elsewhere [8]. As the voltage decreases, the radius of the bubble gradually decreases because of the squeezing force arising from liquid pressure and surface tension. At the voltage of V_c, the bubble is completely annihilated, and the state returns to the *C* state. The temperature of the filament becomes low (at least smaller than 15 K). This gentle process maintains the *I–V* characteristics without a significant current jump in the backward sweep.

To further investigate the mechanism of forward and backward sweeps, the *I–V* loops at different depths were measured at the same ambient temperature. Liquid pressure varies at different depths. The pressure is given by ρgh, where ρ is the helium density, g is the gravitational acceleration, and h is the depth. The depths from 2 to 20 cm correspond to the liquid pressure from 28.5 to 285.0 Pa. To compare our results with previous works [3, 5], we introduce the critical and transition power densities at the filament surface, q_c and q_t corresponding to V_c and V_t, respectively. The critical (transition) power density is calculated from V_c (V_t) multiplied by the current at V_c (V_t), divided by the surface area of the tungsten filament.

Figure 4a shows the forward sweeps at 1.744 K. In the *C* state below V_t, the sweeps almost overlap at different depths, whereas in the *H* state above V_t, the current shows depth dependence, that is, the larger the depth, the higher the current. This indicates that the temperature of the *H* state decreases with increasing depth. We attribute the temperature decrease to the shrinkage of the bubble at higher pressures, resulting in the increase in heat conduction efficiency.

The temperature dependence of filament resistance (R_f) is independently obtained at low power using four-wire measurement. In high temperature range ($T > 50$ K), the temperature dependence of filament resistance (R_f) can be expressed by $T = 19R_f + 3.5$ (K). The R_f will saturate at around 8 K. Therefore, the temperature after transition is estimated about 100 K. As the voltage increases, the temperature will further increase, and the filament start to glow at about 1000 K with 0.8 V.

Notably, V_t and q_t are independent of depth, which are about 146 mV and 0.322 $\mathrm{Wmm^{-2}}$, respectively. The values of q_t are about ten times larger than the

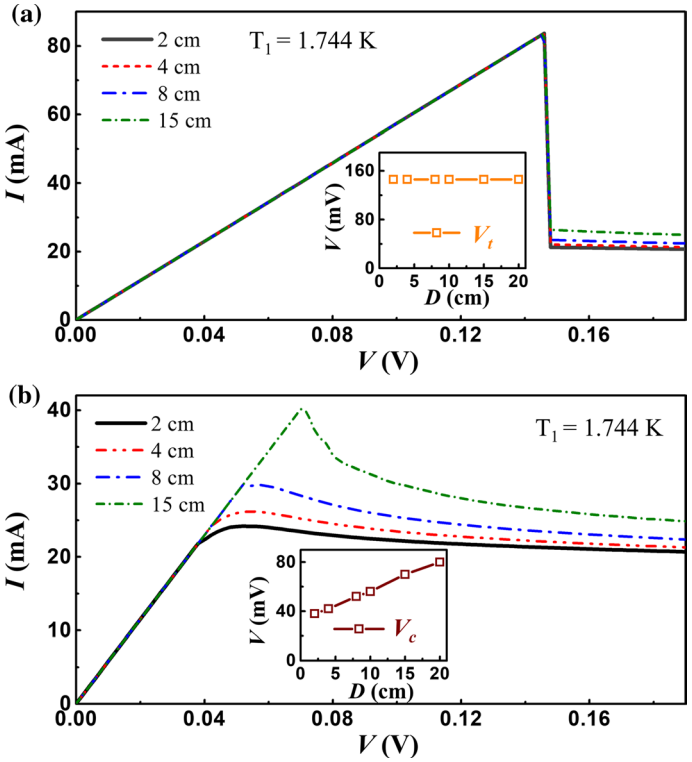

Fig. 4 (Color figure online) **a** *I–V* characteristics of a tungsten filament for forward sweeps at different depths from the liquid helium surface. The inset shows the extracted V_t as a function of depth (D). **b** *I–V* characteristics of a tungsten filament for backward sweeps at different depths from the liquid helium surface. The inset shows the extracted V_c as a function of depth (D)

previously reported values. The huge and depth-independent q_t is inconsistent with that in a previous work [3]. We need to develop a new model to interpret the forward sweep transition, which will be discussed later.

Figure 4b shows the backward sweeps that were also measured at different depths. V_c and the critical power q_c show a positive correlation with depth due to liquid pressure. This behavior agrees with the previous report [3]. Only the backward sweeps show the depth dependence. V_c is always smaller than V_t even at the largest depth. By extrapolating the depth dependence of V_c, the V_c will coincide with V_t at depth of 47 cm at 1.744 K. As the temperature increases, the required depth decreases due to the smaller hysteresis window.

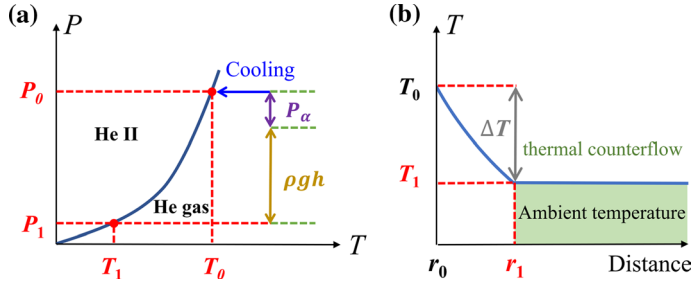

Fig. 5 (Color figure online) **a** Phase diagram for the mechanism of tungsten cooling process. **b** Diagram of the relationship between temperature and distance from the surface of filament

While the thermal conductivity of a superfluid is extremely high in thermal counterflow regime,[1] a significant temperature gradient may exist in the vicinity of the filament surface, which is defined as a thermal boundary layer. Khalatnikov considered the thermal conductivity of superfluid He on the basis of the kinetic theory of elementary excitations [4]. This is totally different from the mechanism of heat transport by the hydrodynamic counterflows of superfluid and normal-fluid components. Figure 5 shows the schematic diagrams of the model employed in Ref. [3]. Figure 5a shows the schematic liquid–vapor phase diagram of liquid He, where T_1 is the ambient temperature and P_1 is the corresponding saturated vapor pressure. P_0 is the pressure necessary to hold a vapor sheath at the surface of the filament. P_0 can be given by

$$P_0 = P_1 + \rho gh + P_\alpha. \tag{1}$$

Here, P_α is the pressure due to the surface tension γ, which is $P_\alpha = \gamma/R$, for a cylindrical sheath of radius R. T_0 is the equilibrium (minimum) temperature necessary for the vapor sheath to exist under P_0. T_0 can be evaluated from P_0 at each depth at the same T_1. Figure 5b schematically explains the temperature gradient from the filament surface to superfluid helium. Here, r_0 is the radius of the tungsten filament and r_1 is the radius at which the temperature equals T_1. Between r_0 and r_1, the thermal conduction is due to Khalatnikov's mechanism [4], and ΔT is the difference between T_1 and T_0.

To quantitatively describe the heat conduction near the filament, we need to have the thermal conductivity of superfluid helium, κ, which is taken from Zinovéva's work [10]. We employ the same functional form as in Ref. [3].

[1] In thermal counterflow regime, the thermal conductivity is still very high even in the quantum turbulence regime. The temperature gradient (∇T) can be estimated by the power density dependent ∇T from Ref. [9]. The maximum ∇T in our experiment is 5.4 Kmm^{-1} under maximum transition power density (0.317 Wmm^{-2}). By integrating ∇T from r_1 to infinity, the temperature different can be obtained as 0.0055 K, which is much smaller compared with the temperature difference within boundary layer.

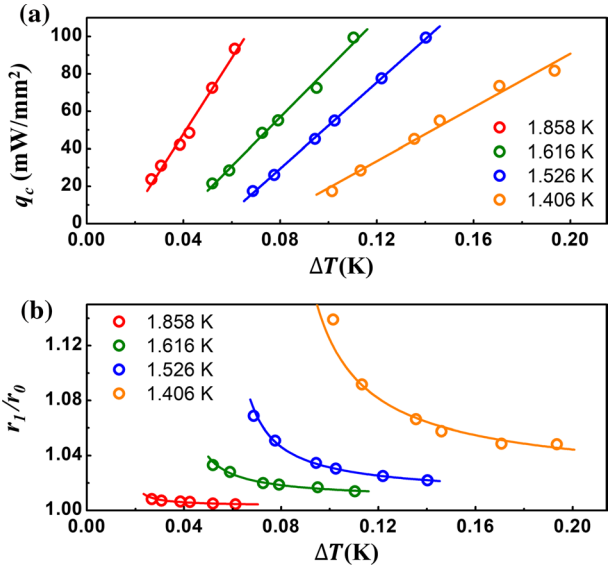

Fig. 6 (Color figure online) **a** Critical power density (q_c) as a function of ΔT under different ambient temperatures. The lines indicate the linear fitting of the data. **b** Ratio of r_1 to r_0 as a function of ΔT at different ambient temperatures. The lines here correspond to the lines in (**a**)

$$\kappa(T) = \kappa_0 \exp\left(-\frac{T}{T_i}\right) \tag{2}$$

Here, κ_0 and T_i are the constants to be determined by fitting, for which we obtained $\kappa_0 = 2.336\ \mathrm{Wm^{-1}K^{-1}}$ and $T_i = 0.367$ K, in the temperature range used in the present work. To describe the heat conduction from the filament, the two-dimensional heat conduction in a cylindrical coordinate should be appropriate. In the cylindrical coordinate, the following Fourier's law of heat conduction holds:

$$\kappa(T)\frac{\mathrm{d}T}{\mathrm{d}r} = -\frac{Q}{2\pi r}, \tag{3}$$

where Q is the total heat flow per unit length. Because the heat is produced only by heating the filament, Q is constant throughout the superfluid He. Using the power density at the filament surface, q(r), we obtain $Q = 2\pi r_0 q(r_0)$. By substituting Eq. (2) into Eq. (3), we can integrate the differential equation as

$$q(r_0) = \frac{\kappa_0 T_i\left[\exp\left(-\frac{T_1}{T_i}\right) - \exp\left(-\frac{T_0}{T_i}\right)\right]}{\ln\left(\frac{r_1}{r_0}\right) r_0}. \tag{4}$$

Then, the ratio of r_1 to r_0 at the critical point ($q(r_0) = q_c$) can be obtained using the measured q_c at each T_1, and T_0 is evaluated from P_0 and T_1 as described above.

Table 1 Fitting parameters of the critical power density

Ambient temperature (K)	A_0 ($WK^{-1}m^{-2}$)	ΔT_0 (K)
2.111	1.80×10^{6}	8.45×10^{-4}
2.022	2.36×10^{6}	7.78×10^{-3}
1.947	2.19×10^{6}	1.02×10^{-2}
1.858	2.03×10^{6}	1.64×10^{-2}
1.744	1.73×10^{6}	2.60×10^{-2}
1.701	1.62×10^{6}	2.97×10^{-2}
1.616	1.31×10^{6}	3.65×10^{-2}
1.574	1.26×10^{6}	4.46×10^{-2}
1.526	1.15×10^{6}	5.46×10^{-2}
1.406	7.17×10^{5}	7.34×10^{-2}

The measured q_c depends on $\Delta T = T_0 - T_1$, as shown in Fig. 6a. A linear relationship can be found, and the coefficients are determined by the least square linear fitting at each ambient temperature. The relationship can be expressed by $q_c = A_0(\Delta T - \Delta T_0)$, where A_0 and ΔT_0 are the coefficients. The fitting coefficients at different temperatures are listed in Table 1. The slope of linear fitting decreases with decreasing ambient temperature, which indicates that q_c is more sensitive at higher temperatures. Note that ΔT shows a finite intersection at q_c equal to zero. Furthermore, in Fig. 6b, we calculate r_1/r_0 using Eq. (4) with the corresponding q_c at different T_0 values at the same T_1. As ΔT increases, the r_1/r_0 becomes less sensitive to ΔT. In Ref. [3], the ratio r_1/r_0 was assumed to be constant. This is true, however, only in the high-power-density region in our present work.

The Kapitza resistance also occurs in this temperature range [11]. Different from our model, the Kapitza resistance is the temperature jump at the interface between a solid wall and liquid helium. For instance, the Kapitza resistance is about 888.4 $KW^{-1}mm^2$ at ambient temperature of 1.526 K obtained from Ref. [11]. The minimum and maximum temperature jump because of the Kapitza resistance for 17.4 and 99.4 $mWmm^{-2}$ are estimated 15.5 and 88.3 K, respectively. These temperatures of filament are too high. The filament resistance increase estimated from the temperature dependence of filament resistance (measured independently) should result in much larger deviation from the linear *I–V* relation in the *C* state. Therefore, the known Kapitza resistance value in this power density region is too large.

Although the *I–V* curve in *C* state is linear, there is a very small variation of about 0.0045 Ω. The upper limit for the temperature of filament in *C* state is then estimated at about 13.5 K. If we attribute this temperature to the Kapitza resistance, the Kapitza resistance is 458 $KW^{-1}mm^2$. Note that this temperature jump due to the Kapitza resistance between the filament and liquid helium does not influence the argument here because all the present analysis is concerning only inside liquid helium.

In Fig. 6a, the finite intersection, ΔT_0, can be extrapolated at each temperature. The temperature difference divided by power density is defined as thermal resistance. It indicates that the thermal resistance may be comparable to the

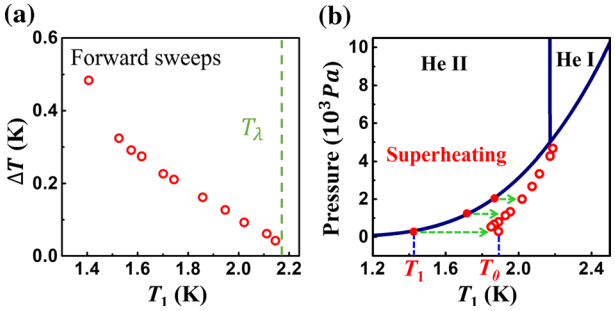

Fig. 7 (Color figure online) **a** ΔT as a function of ambient temperature for forward sweep. **b** T_0 as a function of ambient temperature on phase diagram. The red open circles indicate T_0, and the solid line is the phase boundary

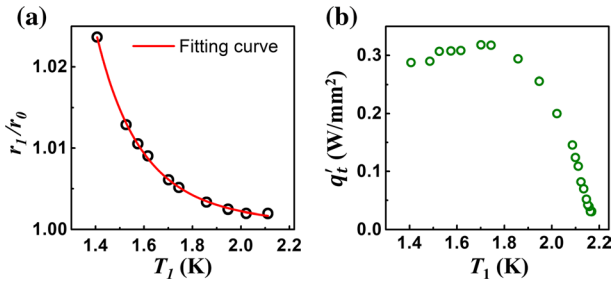

Fig. 8 (Color figure online) **a** Ratio of r_1 to r_0 as a function of ambient temperature. The red line is the least square fitting result. **b** Normalized transition power density (q_t') as a function of ambient temperature

Kapitza resistance when the power density is very low. Note that our model is only valid for the temperature gradient inside liquid helium, so that the ΔT_0 is not the Kapitza resistance which exists between solid and liquid. Nevertheless, the ΔT_0 may be attributed to a part of Kapitza resistance because it cannot be distinguished from each other under usual experimental conditions.

To summarize the backward sweep, our observation reasonably agreed with Ref. [3]. In forward sweeps, the transition power is much larger than the critical power of backward sweeps and is depth-independent. These observations are completely different from the previous work. Although the hysteresis was observed in previous works [3, 5], the hysteresis window was much narrower than the present results. Thus, the transition is not considered to occur at the same liquid–vapor phase boundary shown in Fig. 5a. The transition seems to occur in a metastable superheat state. This phenomenon is similar to the bubble formation in negative-pressure helium [12]. In forward sweeps, ΔT or T_0 may be estimated by extrapolating the relationship between ΔT and q_c (Fig. 6a) to q_t. The extracted ΔT as a function of T_1 is plotted in Fig. 7a. ΔT increases as T_1 decreases, and thus superheating states penetrate into the higher-temperature region at lower ambient

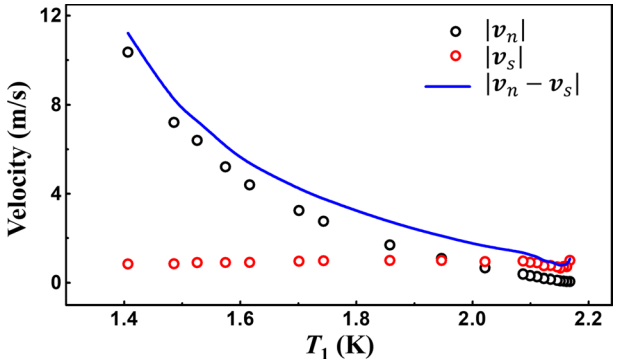

Fig. 9 (Color figure online) Velocities of the normal fluid ($|\mathbf{v}_n|$), the superfluid component ($|\mathbf{v}_s|$), and relative counterflow velocities ($|\mathbf{v}_n - \mathbf{v}_s|$) as a function of ambient temperature

temperatures. As shown in the phase diagram in Fig. 7b, each T_1 corresponds to one T_0 because of the depth independence. We attributed the bubble formation over the tungsten filament to the superheat limit.

The r_1/r_0 of forward sweeps is calculated from ΔT (T_0) in Fig. 7b using Eq. (4), as shown in Fig. 8a. By comparing with backward sweeps, we find that the value of r_1/r_0 of forward sweeps is smaller, which is consistent with the trend observed in Fig. 6b. We fit the relationship between r_1/r_0 and T_1 to find an empirical expression as $r_1/r_0 = 0.3T_1^{-7.5} + 1$.

The effective transition power density q_t' can be calculated by assuming an effective surface area at radius r_1, beyond which a thermal counterflow regime is restored. Figure 8b shows q_t' as a function of T_1. q_t' increases as T_1 decreases at temperatures near T_λ. However, owing to the increase in r_1 at low temperatures, q_t' has a maximum value of 0.317 Wmm^{-2}.

From Landau's two-fluid model [13], a superfluid consists of a superfluid component and a normal component. The superfluid component is in the macroscopic quantum ground state, which carries no entropy and has no viscosity. Only the normal component carries entropy and heat. To explore the hydrodynamic properties, the density and velocity field of the superfluid component (normal component) are defined as ρ_s (ρ_n) and $\mathbf{v}_s(\mathbf{v}_n)$, respectively. The total density of fluid is determined by $\rho = \rho_s + \rho_n$. The total flux of the mass flow is $\mathbf{j} = \rho_s\mathbf{v}_s + \rho_n\mathbf{v}_n$. In the thermal counterflow regime, since there is no net mass flow ($\mathbf{j} = 0$), the heat flux (power density) $\mathbf{q}$ can be described by

$$\mathbf{q} = \rho s T \mathbf{v}_n, \tag{5}$$

where s is the entropy of helium. The velocities $\mathbf{v}_n$and $\mathbf{v}_s$ are obtained using Eq. (5) with q_t'. The counterflow velocity $v_{cf} = |\mathbf{v}_n - \mathbf{v}_s|$ can be calculated. As shown in Fig. 9, $\mathbf{v}_n$ dominates approximately below 2 K. Note that v_{cf} is larger than the typical critical velocity of quantum turbulence. Nonetheless, there is no indication of critical velocity for the mechanism of vapor sheath formation around the tungsten

filament in the forward sweep. We attribute the transition mechanism in the forward sweep to the superheat limit, although its details should be studied further.

In previous works, an audible hiss was heard [3, 5]. This phenomenon is also referred to as turbulence. In our experiment, no hiss was heard. It was reported that the hiss appeared in a certain intermediate range of power density [5]. In these previous works, a straight linear filament was used, whereas our filament was coiled. Hence, the bubble shape in these previous works should be cylindrical instead of spherical. The cylindrical bubble may develop an instability similar to Rayleigh instability, which develops on a cylindrical liquid [14]. The hiss may be attributed to such an instability.

4 Summary and Conclusion

In summary, we clearly defined the V_t and V_c as the transition and critical voltage for forward and backward sweeps of the tungsten filament, respectively. A temperature dependence of the *I–V* hysteresis loop of the tungsten filament in superfluid helium is reported here for the first time. The maximum hysteresis window was about 100 mV with power density difference of about 0.282 Wmm^{-2}. For analyzing the backward sweeps, the model of the thermal transport in the vicinity of the filament reported by Date et al. was employed [3]. The diffusion of elementary excitations results in a temperature gradient of the thermal boundary layer was described, but we further revised the theory with additional surface tension to explain the condition more properly. The extracted r_1/r_0 or thickness of boundary layer of backward sweeps showed depth dependence, which is different from a previous report [3]. As temperature difference between filament surface and liquid (ΔT) increased, the r_1/r_0 gradually decreased to a constant value at each ambient temperature. Furthermore, the critical power density exhibited a linear relationship with ΔT. Specifically, in forward sweeps, the transition power density was independent of depth; thus, we described the phenomena as being due to the superheating mechanism. The ΔT of forward sweeps was obtained by extrapolating the linear relationship of the critical power density and ΔT with the transition power density. Each ambient temperature corresponds to a ΔT for forward sweeps, and the ΔT increases as ambient temperature decreases. Moreover, the r_1/r_0 of forward sweeps was calculated from ΔT. The r_1 under each ambient temperature was utilized to normalize the transition power density, which shows a maximum value of 0.317 Wmm^{-2}. The velocities of the normal fluid, superfluid component, and counterflow were estimated. The $\mathbf{v}_{cf}$ at forward transition point is not constant at different temperatures. This implies no critical velocity for the mechanism of this transition. The value is larger than the usual $\mathbf{v}_{cf}$ of quantum turbulence. It is interesting to further study the Kapitza resistance under high power density and the finite ΔT shown in Fig. 6a and Table 1.

Acknowledgements We are indebted to Professor Ming-Chiang Chung for helpful suggestions and comments. We are grateful to Professor Ben-Li Young for help with setting up the cryogenic apparatus. KK thanks Professor Jenh-Yih Juang for his kind hospitality. We thank Prof. P Leiderer for helpful discussion about imaging bubbles. This work was supported by the Ministry of Science and Technology, Taiwan,

ROC, under Grant No. MOST 108-2122-M-009-013. KK was supported by JSPS KAKENHI Grant Number JP17H01145 and the Program of Competitive Growth of Kazan Federal University.

Compliance with Ethical Standards

Conflict of interest The authors declare that they have no conflict of interest.

References

1. N. Yadav, P.K. Rath, Z. Xie, Y. Huang, A. Ghosh, J. Low Temp. Phys. pp. 1–18 (2020)
2. M. Ashari, D. Rees, K. Kono, E. Scheer, P. Leiderer, J. Low Temp. Phys. **167**(1–2), 15 (2012)
3. M. Date, H. Hori, O. Ichikawa, J. Phys. Soc. Jpn. **35**(4), 1190 (1973)
4. I.M. Khalatnikov, *An Introduction to the Theory of Superfluidity*, 1st edn. (CRC Press, Boca Raton, 2000). https://doi.org/10.1201/9780429502897
5. J.S. Vinson, F.J. Agee Jr., R.J. Manning, F.L. Hereford, Phys. Rev. **168**(1), 180 (1968)
6. C.C. Shih, M.H. Huang, P.C. Chang, P.W. Yu, W.B. Jian, K. Kono, Current bistability of a tungsten filament in superfluid helium-4. Submitted
7. I.F. Silvera, J. Tempere, Phys. Rev. Lett. **100**(11), 117602 (2008)
8. C.C. Shih, M.H. Huang, P.C. Chang, P.W. Yu, W.B. Jian, K. Kono, To be submitted
9. C.E. Swanson, R.J. Donnelly, J. Low Temp. Phys. **61**(5–6), 363 (1985)
10. K. Zinoveva, J. Exp. Theor. Phys. USSR **4**(1), 36 (1957)
11. R.C. Johnson, W. Little, Phys. Rev. **130**(2), 596 (1963)
12. H. Maris, S. Balibar, Phys. Today **53**(2), 29 (2000)
13. L.D. Landau, E.M. Lifshitz, *Fluid mechanics* (Pergamon Press, 1979), vol. 6, chap. XVI, pp. 507–522
14. L. Rayleigh, Philos. Mag. **34**(207), 145 (1892)